# Thermo-mechanical response of Cu foils for microsystems

G. Khatibi[1,4], V.Gröger[1], H.Merchant[2], B.Weiss[1] and R.Wiechmann[3]
[1]Institute of Materials Physics, University of Vienna, Vienna, Austria
[2]Gould Electronics, Eastlake, Ohio, USA
[3]Gould Electronics, Eichstetten, Germany
[4] Institute of Physical Chemistry, University of Vienna, Vienna, Austria

**Abstract**
Electrodeposited copper foils of different grain sizes (due to different deposition parameters) and rolled foils, all with identical thickness of 35 µm, have been thermally treated and investigated by displacement controlled tensile tests at a strain rate of $5 \times 10^{-5}$/s. For the strain measurements at temperatures up to 300°C a microtensile tester in combination with a laser speckle sensor has been used. Young's modulus was obtained from averaging loading-unloading paths at several strain levels. The room temperature elastic parameters for the electrodeposits are strongly reduced compared with a bulk sample of average texture and decreases drastically at higher testing temperatures presumably due to clustering of the high concentration vacancy-type defects. In the elasto-plastic and plastic region the critical yield stress, the strain hardening coefficient and the stress for 1% strain correlate well with grain size. For the stresses a Hall-Petch-type relationship holds due to a combination of direct and indirect grain size influences.

## 1. Introduction

Electrodeposited copper foils are frequently used as parts of microelectronics and MEMS of high reliability under conditions of mechanical and thermal cycling (1). As the mechanical and thermal properties of such foils depend strongly on the material structure (size and boundaries of grains and subgrains, twins, texture, specific defects, additives) resulting from the particular deposition process (2,3), they may be surprisingly different from reference values obtained for bulk copper. Thus systematic experimental data are needed as input for finite element calculations of the MEMS performance and consequently for an optimization of the foil properties with this respect. Electrodeposition produces characteristic defects considerably different from the defects generated by rolling. Due to the transition from an epitaxial to a dominant texture of columnar grain clusters at a critical thickness deformation twins form. The defect density in the grain boundary is strongly reduced and specific grain boundary structures are generated. Additionally, hydrogen evolved at the cathode is trapped at the vacancy type defects thus hindering vacancies from annealing and preventing vacancy clusters from collapsing into loops and from annealing out at the grain boundaries (2). Thus vacancies and vacancy-type defects are produced up to concentrations of 1%. Gas filled voids are strong obstacles for dislocation motion. The defect concentrations, the crystallographic textures perpendicular to the substrate plane as well as the grain sizes are governed mainly by the excess of the deposition potential over the equilibrium value (overpotential) and the surface active electrolytic additives. Schematics for these structural features (2) are shown in Fig.1. Columnar grain clusters, grain sizes and voids are shown in a sample cross-section (Fig.1a) perpendicular to the deposition plane as accessible by optical microscopy, the specific sites where voids are preferentially generated are given in Fig.1b. The void concentration will thus be inevitably connected with the grain size. In the mid-thickness in-plane section (investigated by TEM) twin arrangements are shown schematically (Fig.1c), as well as subgrains, coherent domains and dislocation arrangements (Fig.1d). Again twin density, dislocation density and subgrain boundary structure are connected with the grain size.

This investigation aims to compare mechanical properties of various electrodeposited and rolled samples with identical thickness but different grain size as function of test temperature (and relate

them to bulk values). Special emphasis was placed on the microstructural differences between the samples, especially texture. The wealth of systematic knowledge about the structure of these electrodeposits (2-6) will be used as additional source. For stabilizing the structures annealing at 180 °C (at similar conditions as in Cu/FR-4 laminating process) is carried out, sharpening subgrain boundaries, coarsening the vacancy loops and increasing the grain size, while twin structures remain essentially unchanged. The kinetics of recrystallization in electrodeposited samples is governed by the high concentration of vacancy-type defects as can be concluded from the low activation energy of about 0.6 eV (5,6). Thus considerable grain growth can occur dependent on the structural instability being larger for samples with smaller grains.

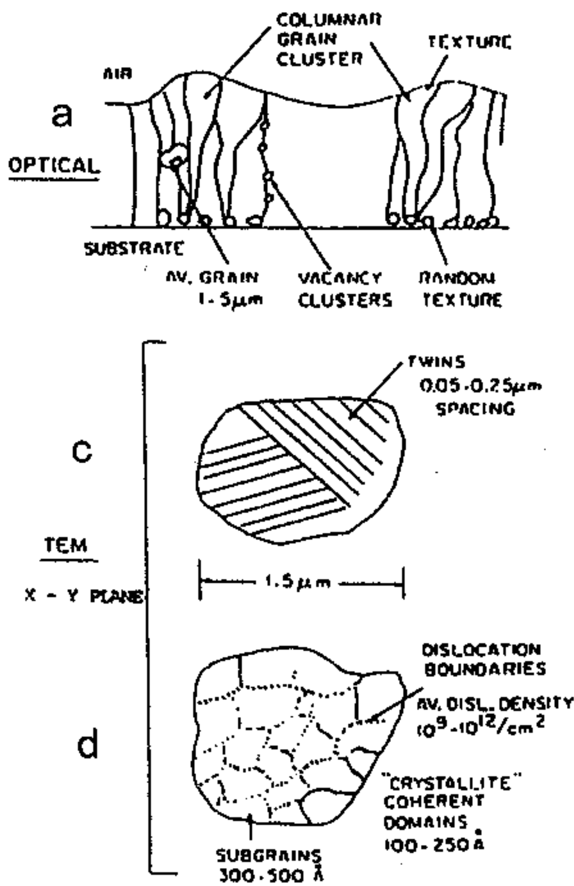


Figure 1: Schematic of Structure of Electrodeposit:
a) Cross section perpendicular to plane normal
b) voids produced at:
1 .. grain boundaries, 2 .. growth steps, 3 .. morphological valleys
c) Twins, d) Subgrains and coherent domains: in mid-thickness plane as seen by TEM (2)

Elastic and plastic properties of thin foils are not readily acccessible in tensile tests by conventional experimental techniques measuring the strain by means of crosshead motion. This investigation makes use of a laser speckle technique for contactless strain measurements in tensile tests to determine Young's modulus, critical yield strength values, strain hardening parameters and yield strength at 1% strain in comparison of electrodeposits of different grain sizes and rolled foils.

## 2. Experimental

Variously prepared electrodeposited foils stripped from chromium substrate and a rolled foil were subjected to an annealing treatment for 30 minutes at 180°C. From different sections the textures

have been determined. The electrodeposited foils show columnar grain clusters with strong textures in the direction normal to the deposition plane. The textures are changing gradually from a epitaxial random texture to the dominant texture <220>. The in-plane texture (determined from the mid plane) influencing all mechanical properties determined by straining in plane was completely random. In contrast to that the rolled foil showed an in-plane texture of the type <100> and <111>. The resulting in-plane grain sizes for the electrodeposited foils have been determined from planar TEM investigations from which the detailed size distributions can be deduced (see also (6)). Optical microscopy was used to describe the cross-section perpendicular to the substrate plane for all foils. The characteristic microstructural features and the textures are summarized in Table1. One has to bear in mind that increasing grain sizes of deposits occur together with increasing twin spacing and reduced concentration of vacancy-type defects. The structures obtained are far from being in equilibrium, the instability being strongest in the most fine-grained sample. Vacancies and small vacancy clusters play an important role in that case as can be concluded from the still reduced activation energy if temperatures up to 250 °C are considered (5).

Table1: Characterization of the copper foils (thickness 35 µm, thermal anneal 180°C for 30 min)

| Foils | Chemical Comp. | Microstructure | Grain size (µm) | | Texture | Remarks |
|---|---|---|---|---|---|---|
| | | | before | after testing at 300°C | | |
| AM | 99,99 | Equiaxed, no growth twins ▶ disl. density | 0,3 | 2 | Random in (z) and in x-y planes | High point defect conc. near GB and in GB 0,1%, vacancy clusters, microvoids, gas bubbles |
| GR 3 (high profile) | 99,99 | Columnar morphology // z, numerous growth twins x-y plane equiaxed | 2 | 2-3 | <220> fibre in z x-y plane: random | |
| GR 3 (low profile) | 99,99 | few growth twins x-y plane equiaxed | 0,5 | 2 | <220> fibre in z x-y plane: random | |
| GR 8 (rolled) | 99,9 (> 100 ppm Oxygen) (ETP grade) | pancaked in the x-y plane, disl. cells, subgrains | 4,5 | 30-40 | Mixed <100> plus <111> in x-y plane | Large flattened as-cast grains, highly anisotropic microstructure |

All mechanical data (see also 7) have been obtained using a microtensile tester making use of special grips and a laser speckle strain sensor being described in detail elsewhere (8). The measurement principle is shown schematically in Fig. 2.

During a displacement controlled tensile test at a strain rate of $5 \times 10^{-5}$/sec the sample is illuminated by two collimated laser beams of a few mW power and laser speckle patterns are recorded by two CCD sensors representing two sample surface spots separated by a base length of 20 mm. The shifts are obtained on-line from the cross-correlation function between subsequent images. From the differential shift and the base length the strain is evaluated (8). A strain resolution of about $2 \times 10^{-5}$ can be achieved.

For determination of Young's modulus, the initial slope is usually not accessible for such thin samples due to inevitable imperfections of mounting. Thus for determinations of Young's modulus an unloading/reloading technique was used during the tensile test. Young's modulus was obtained from the average slopes of the respective curve portions which were in accordance with an error smaller than 5 %. Due to the lower general stress level and some creep influence the errors are higher with increasing temperatures up to 10% at 300°C. Additionally the following parameters

were obtained from tensile tests: critical yield stress σ(0,02%), yield stress σ(1%) and tangent modulus $E_T = d\sigma/d\varepsilon$ as function of strain in the same strain range. A regulated air furnace allowed to control the sample temperature. Tests have been carried out at temperatures up to 300°C. Depending on the temperature the required heating time to reach the desired testing temperature was up to about 20 minutes. During this period and the tensile test (about 5 minutes) structural changes occurred being largest for 300°C measuring temperature. The grain size enhancement also given in Table 1 is largest for the fine-grained sample due to its greater instability. For each condition five individual samples were tested and data averaged.

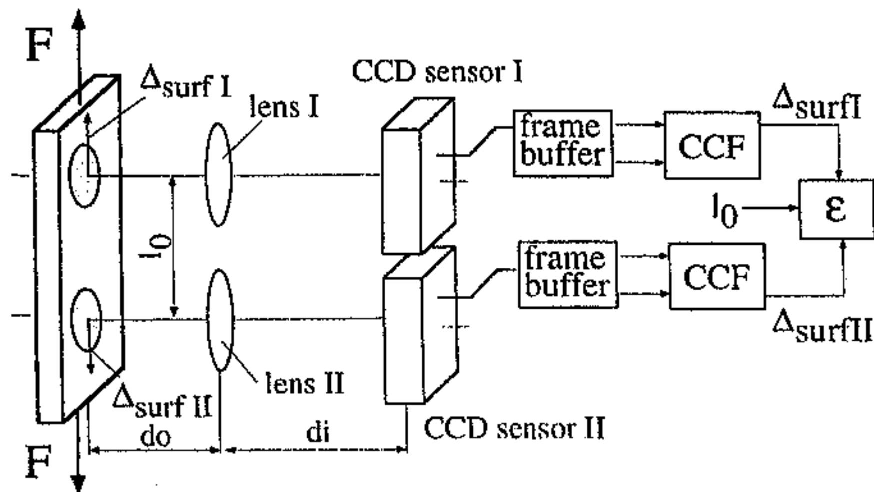


Figure 2: Schematic of laser strain sensor (8)

**3. Results and discussion**

a) Elastic property: Young's modulus

The results for Young's modulus are shown for four samples as function of temperature in Figure 3. The grain sizes for the preannealed material and additionally the grain sizes after the end of the 300°C experiment are indicated. All values are decreasing with temperature the rate being stronger for the smaller grains.

Young's modulus in copper varies strongly with crystal orientation and has an average value for defect-free copper of about 125 GPa at room temperature. This value can be influenced by defects. In particular porosity and cracking reduce the values (9, 10). Vacancies can have a slight reducing effect (11) which is due to an elastic, an anelastic and a pinning contribution opposing one another (12). A temperature rise to 300°C reduces the modulus by about 11% (13).

Interpreting at first the room temperature results the value of about 98 GPa for the rolled sample can well be due to the specific sample texture. The texture of the electrodeposits is random. From the rather low-density grain boundary structures together with the vacancy-type defects Young's modulus after deposition must be considerably reduced (compared with 125 GPa), the resulting value should be lower the more fine-grained the sample is. The initial anneal for 30 minutes at 180°C stabilizes the grain structure so that a recovery of Young's modulus towards higher values should occur. It seems that the faster kinetics due to the larger vacancy concentrations leads to such a strong recovery so that the values of the fine grained samples are higher after annealing. Nanocrystalline copper produced by severe plastic deformation under hydrostatic stress has a much

stronger grain boundary structure and consequently shows smaller changes of Young's modulus (14, 15).

The temperature dependence can be only in part attributed to a direct temperature dependence of Young's modulus (possibly below 100°C). At the higher temperatures structural changes must have a strong influence. Again, the concentration of the surviving vacancy-type defects are responsible for differences in annealing kinetics. Thus the values for the electrodeposits show a steeper slope than the rolled sample and decrease to lower values, the strongest structural change occurs for the smallest grain sizes. This additional decrease to about half the value indicates a dramatic softening of the structure absent in mechanically prepared nanocrystalline copper (14, 15). The cause can only be attributed to the voids, agglomerated at the grain boundaries. The electrodeposits could be weakened further by microcracks at the voids as quasi-elastic annular flaws (10) possibly initiated at the largest voids. The cause can only be attributed to the voids, agglomerated at the grain boundaries. The electrodeposits could be weakened further by microcracks at the voids as quasi-elastic annular flaws (10) possibly initiated at the largest voids.

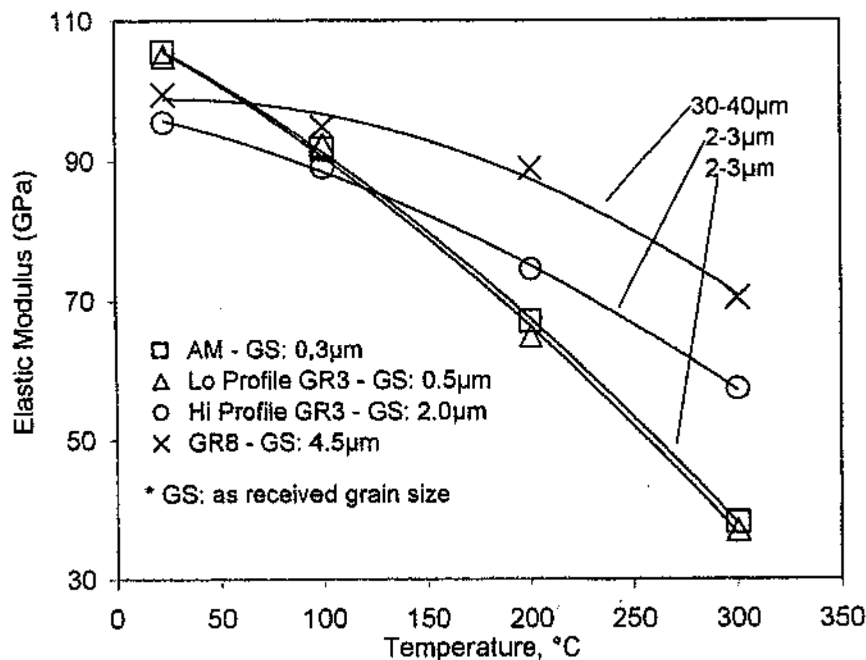


Figure 3: Influence of test temperature on Young's modulus for copper foils of 35 µm thickness (AM and GR3 electrodeposits, GR8 rolled foil). The grain sizes after the 300°C test (right insert) differ form the initial ones (left insert) due the microstrtructural instabilities.

b) Elasto-plastic and tensile properties

In Figure 4 the results are shown for the critical yield stress $\sigma(0{,}02\%)$ and for the stress at 1% deformation $\sigma(1\%)$ as function of deformation temperature (and the concomitant structural change). At room temperature the values correlate well with grain size. As the smaller grains have also a higher density of vacancy-type defects, an increase of the flow stress achieved by the direct influence of grain size. Thus a Hall-Petch plot is quite nicely met as can be seen in Fig.5. The gradual reduction of stresses with temperature may be due to an influence of dislocation motion (thermally influenced) nearly independent of the initial grain size. Further the reduction of the stress values may also be due to grain growth and other structural changes which are influenced by the various concentrations of vacancy type defects present. The strongest structural changes occur for

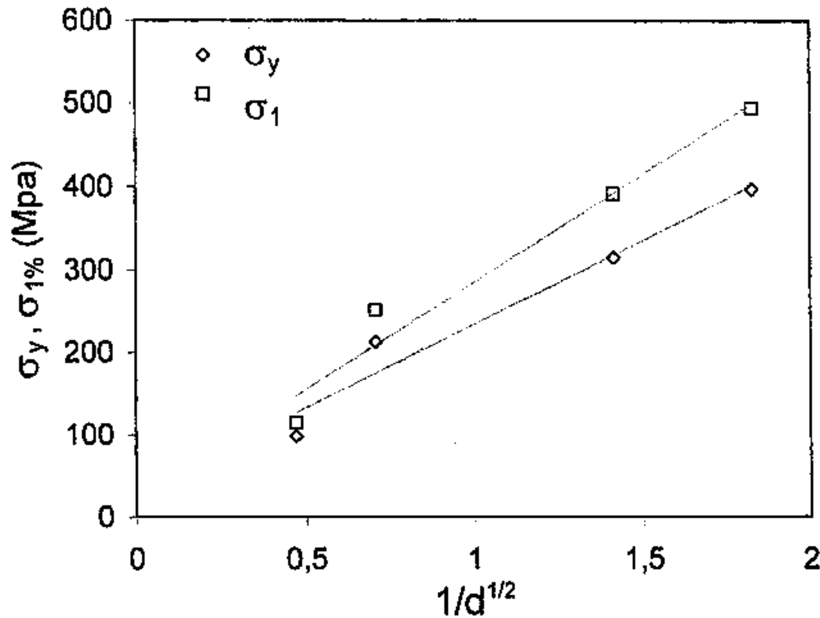


Figure 5: Hall-Petch plot for stress values σ(ε= 0.02%) and σ(ε=1%)

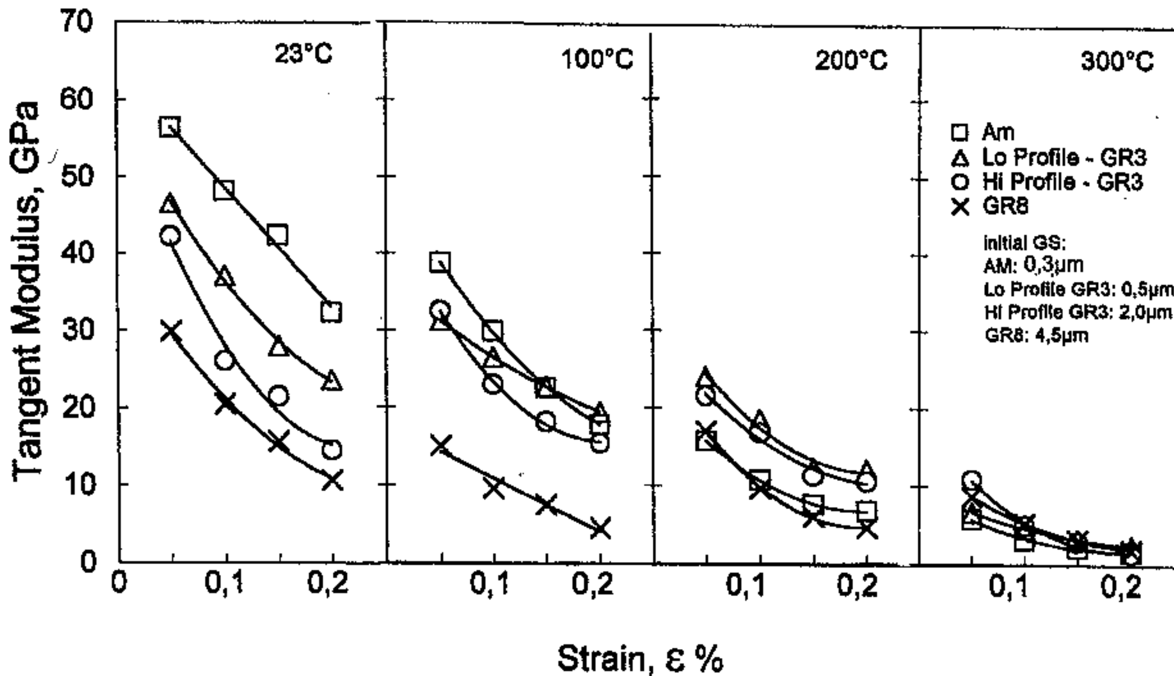


Figure 6: Effect of Strain and Temperature on Tangent Modulus for 35 µm Copper Foils

**4. Summary**

A system for uniaxial testing of thin foils with a tensile tester making use of a laser speckle strain sensor of high strain resolution is introduced and applied. The dependence of elastic and plastic properties of electrodeposited copper foils of different grain size show that the defect structure, especially the grain boundaries and the high vacancy concentration of electrodeposits, is responsible for the mechanical properties. Comparing foils stabilized at 180°C for 30 min of different grain sizes in their room temperature performance, the foil with the smallest grain size (300 nm) shows the highest values of Young's modulus, critical yield stress, hardening coefficient and stress at 1% strain. Due to the larger instability this advantage of performance of the small grained samples vanishes totally and is even turned into a disadvantage if the samples are loaded at 300°C.

the smallest grain size connected initially with the highest vacancy concentration with the result that at 300°C the grain sizes of all electrodeposits become very similar. Consequently the curves tend to converge. There are only gradual differences for the curves shown for the two different strains. For a clarification of the strain influence near the critical yield stress the tangent modulus was plotted in Fig.6 as function of strain in the range 0,05 to 0,2. Additional to a general decrease in level again due to thermal activation the relative shifts of the curves indicate clearly the different rates of structural changes. The curve for the sample with the finest grains is shifted gradually from the top position at 23°C measuring temperature to a bottom position at 300°C where again the curves tend to coincide.

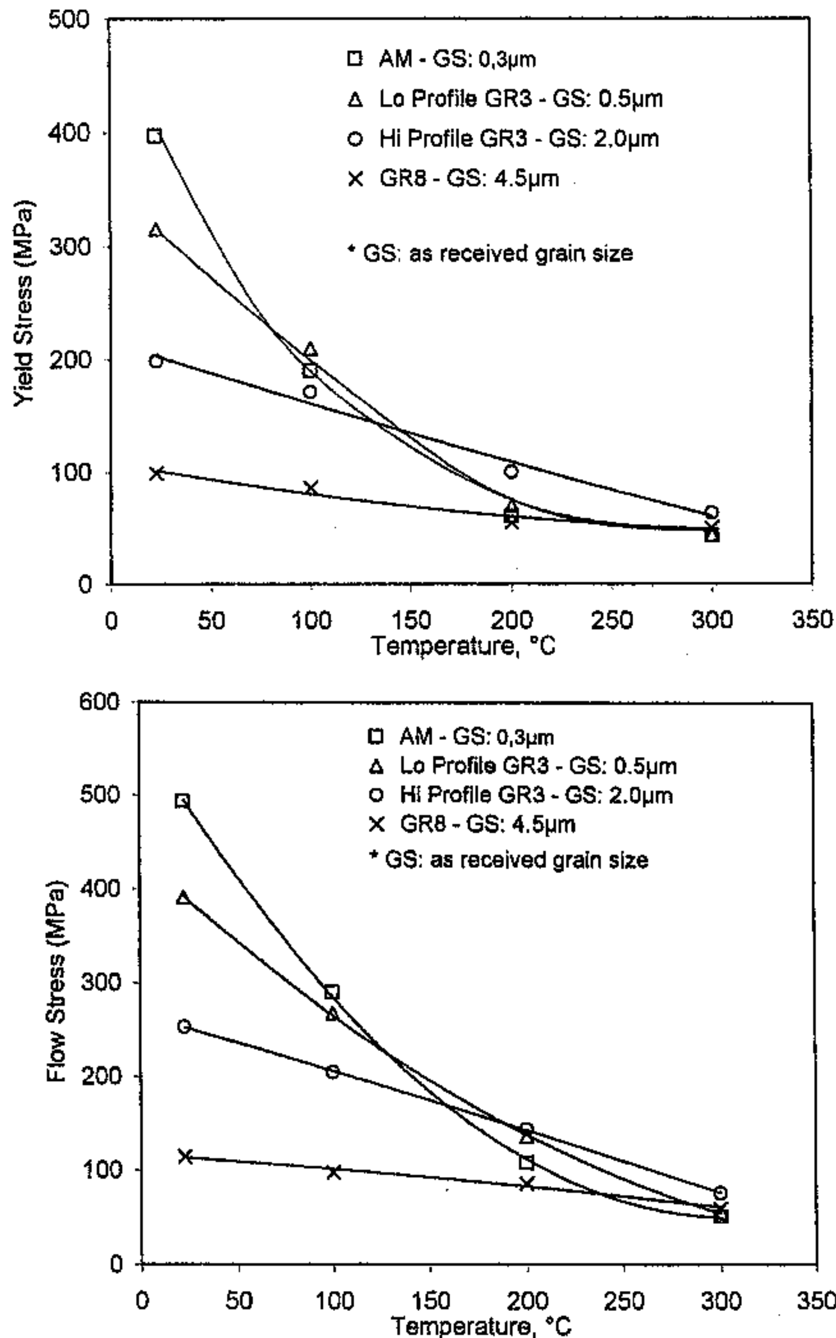


Figure 4: Effect of Temperature on Yield Stress and Flow Stress (at1% Strain) for 35µm Copper Foils

**5. Acknowledgement**
The authors thank the Fonds zur Förderung der wissenschaftlichen Forschung, Wien (P 12311 TEC And P14732 TEC) for financial support. SEM characterisation of the foils by Prof. Dr.R.Stickler is acknowledged.

**6. References**

1. B.Michel and T.Winkler eds., Proc.Int.Conf. Micromaterials, MicroMat2000, DVM Berlin 2000
2. H.D.Merchant in Defect Structures, Morphology and Properties of Deposits, ed.H.Merchant, The Minerals; Metals and Materials Society (1995) 1-
3. H.D.Merchant and O.Girin: MRS Proc.431 (1997) 433-
4. H.D.Merchant: J.Electron.Mat.22 (1993) 631-
5. H.D.Merchant: J.Electron.Mat.24 (1995) 919-
6. H.D.Merchant and M.G.Minor: J.Materials Science, in preparation
7. G.Khatibi, M.Klein, E.El-Magd, H.D.Merchant, B.Weiss, R.Wiechmann and P.Zimprich: Proc.IPC EXPO 2001, Anaheim, CA, April 2001
8. M.Anwander, B.Weiss,B.Zagar and H.Weiss in Experimental Mechanics, ed.I.M.Allison, Balkema, Rotterdam (1998) 692 -
9. F.P.Knudsen:J.Amer.Ceram.Soc. 45 (1962) 94-
10. V.Krstic, U.Erb and G.Palumbo:Scripta Met. 29 (1993) 1501-
11. Gmelin, Handbuch der anorg.Chemie Teil A, 8.Aufl. (1955) 850-
12. J.R.Townsend, J.A.DiCarlo,R.L.Nielsen and D.Stabell: Acta Met. 17 (1969) 425-
13. D.Lazarus: Phys.Rev 76 (1949) 545-
14. A.B.Lebedev, Yu.A.Burenkov, S.A.Pulnev, V.V.Vetrov and V.I.Kopylov: J.Phys. IV, C8 (1996) 365-
15. I.V.Aleksandrov, R.M.Mazitov, A.R.Kil'mamelov, K.Zhang, K.Lu and R.Z.Valiev: Phys.Met.Metallogr.90 (2000) 164-